

First Principle Study to Correlate Location and Activity of Ruthenium Oxide Incorporated in Alkali-Metal Hexatitanates

Abhijit Chatterjee,* Hiromichi Hayashi, and Takashi Iwasaki

Inorganic Materials Section, Tohoku National Industrial Research Institute, 4-2-1 Nigatake, Miyagino-ku, Sendai 983-8551, Japan

Received: October 31, 2000; In Final Form: February 27, 2001

Ab initio total energy pseudopotential calculations were performed on ruthenium oxide incorporated alkali-metal hexatitanates to study the location and activity of ruthenium oxide. The influence of alkali metals on the activity is also monitored. The photocatalytic activity of alkali-metal hexatitanates in the presence of ruthenium oxide increases in the order $\text{Na} > \text{K} > \text{Rb}$. To rationalize the role of the hexatitanate structure on its activity, both ruthenium oxides incorporated and unincorporated structures were investigated. One objective is to monitor whether the ruthenium oxide incorporated in the tunnel has photocatalytic activity or not. The present results suggest that the tunnel structure in the Na-hexatitanate framework is well suited for accommodating Ru species and induces strong interaction between the active species and the host oxide. Density of state calculations were performed on both structures (with and without ruthenium oxide) to verify the activity of ruthenium oxide. It is observed that ruthenium oxide residing in the inner tunnels of the hexatitanate structure plays an active role in photocatalysis. A novel methodology has been formulated to explore other complicated inorganic materials of interest.

Introduction

Alkaline metal hexatitanates $\text{M}_2\text{Ti}_6\text{O}_{13}$ ($\text{M} = \text{Na}, \text{K}, \text{Rb}$) have a rectangular tunnel structure. These relatively cheap fibrous materials have thermal stability, chemical resistivity, and dispersibility. These properties make it possible for the usage of these compounds as reinforcing material for plastics, heat-insulating paints, and filter materials.^{1,2} The structure of these type of materials is such that an octahedral of TiO_6 shares edges at one level in linear groups of three.³ Each is joined above and below to similar groups by further edge sharing to form an open octahedral framework enclosing tunnels, in which the sodium ions are located. The tunnel structure of these materials has generated immense interest in its application as photocatalysts. These alkali-metal hexatitanates hence act as semiconducting photocatalysts capable of invoking a photocatalytic decomposition of water to produce hydrogen and oxygen.^{4–7} The photocatalytic activity for water decomposition of these hexatitanates depends on the type of alkali metal atom, M , and increases in the order $\text{Na} > \text{K} > \text{Rb}$. Now, when Ru ions were intercalated through ion exchange with alkali-metal ions in the titanates and were favorably activated by oxidation rather than reduction treatment, they have a capability of stoichiometric production of hydrogen and oxygen.⁸ It has been proposed that the framework of the tunnel structure is responsible for the activity. A recent study⁹ has shown that dispersion of RuO_2 over hexatitanates enhances the photocatalytic activity manifold. It has been pointed out that the usefulness of tunnel structure of the titanates for photocatalysis is based on the presence of internal electrostatic fields and the formation of highly dispersed RuO_2 particles. A correlation between the concentration of the O^- radical and photocatalytic activity was established, thus indicating that the O^- radical probably works as a hole site in

the photocatalysis reaction, and the ability to separate photo-excited charges reflects the photocatalytic activity order of $\text{M}_2\text{Ti}_6\text{O}_{13}$. Now, the structure and the role of ruthenium oxide particles inside hexatitanates are yet to be known. Whether the ruthenium oxide staying inside the tunnel structure has any photocatalytic activity is yet to be resolved.

Until recently, the understanding of bulk, surfaces, and interfaces of oxides lagged far behind than that of semiconductors and metals. This was partly due to experimental difficulties and partly because the complexity of many oxide materials made them difficult to study with accurate theoretical methods. Early ab initio calculations on the energetics and relaxed structure of an oxide surface were made on $\text{MgO}(001)$ using HF (Hartree–Fock) theory,¹⁰ and HF calculations have since been used on several other oxides.^{11–15} The DFT (density functional theory) method began its venture in oxides somewhat later but progressed at rapid speed and a number of studies have been reported in the past decade on oxides as well as other materials.^{16–23} In the last three years there has been a lot of progress in this area.^{24–28} There are two very recent works^{29,30} on the electronic and structural properties of mixed metal oxides using first principle density functional theory. We also used density functional theory to correlate layer charge and catalytic activity of dioctahedral smectites.³¹ There are so far no studies related to the alkali-metal titanates.

The primary aim of the present investigation is to correlate location and activity of ruthenium oxide intercalated in alkali-metal hexatitanates. To achieve this, one has to first rationalize the equilibrium position of alkali-metal cations in hexatitanates, which will then be compared with the existing crystallographic results to validate the model and the reliability of the current theoretical methodology. Then we use localized cluster models to trace the favored orientation of isolated ruthenium oxide in the hexatitanates and also monitor the dependence of the alkali metals on the location of ruthenium oxide. This step also helps

* Corresponding author. Phone: +81-22-237-5211. Fax: +81-22-236-6839. E-mail: chatt@tniri.go.jp.

to propose and validate the ruthenium oxide inclusion mechanism. A periodic first principle study with ruthenium oxide incorporated inside the tunnel of the hexatitanate is then carried out using the geometry obtained from the cluster calculation. We will discuss the situations with incomplete ion exchange (alkali metals are present along with ruthenium oxide) and complete ion exchange of alkali-metal cation by ruthenium oxide (all alkali metals available has been exchanged by ruthenium oxide). Then the experimental trend of photocatalytic activity is examined. The density of state (DOS) calculations over hexatitanates justify the role of ruthenium oxide in photocatalysis. A plausible mechanism for the activity of ruthenium oxide is proposed. The novel methodology based on DFT has thus been rationalized.

Method and Model

Ab initio total energy pseudopotential calculations were performed using CASTEP (Cambridge Serial Total Energy Package), which has been described elsewhere^{32,33} and associated programs for symmetry analysis were used. In this code, the wave functions of valence electrons are expanded in a basis set of plane waves with kinetic energy smaller than a specified cut of energy ' E_{cut} '. The presence of tightly bound core electrons is represented by nonlocal ultrasoft pseudopotentials.³⁴ Reciprocal space integration over the Brillouin zone is approximated through a careful sampling at a finite number of k points using the Monkhorst-pack scheme.³⁵ The exchange-correlation contribution to the total electronic energy is treated in the generalized gradient corrected (GGA) form³⁶ of the local density approximation (LDA). In all calculations, the kinetic energy cutoff E_{cut} and the density of the Monkhorst-Pack k -point mesh were chosen high enough in order to ensure convergence of the computed structures and energetics. To obtain equilibrium structures for a given set of lattice constants, ionic and electronic relaxations were performed using the adiabatic or 'Born-Oppenheimer' approximation, where the electronic system is always in equilibrium with the ionic system. Relaxations were continued until the total energy had converged.

All the cluster calculations have been performed with DFT³⁷ using the DMOL code of MSI Inc. BLYP^{38,39} exchange correlation functional and a DNP basis set⁴⁰ were used throughout the calculations.

The structures of the sodium and rubidium hexatitanates were generated using the crystal structure data of Andersson et al.³ and that of potassium hexatitanate was generated using the data of Berry et al.⁴¹ One unit cell of the structures was chosen and fully relaxed. The general structure of an alkali-metal hexatitanate with the alkali-metal cation being sodium is shown in Figure 1. This is followed by the incorporation of ruthenium oxide at the crystallographic position of two alkali-metal ions (i.e., two of the alkali-metal ions are replaced by Ru and O atoms of ruthenium oxide). The structures after ruthenium oxide incorporation were also optimized. The relaxations of ions to calculate the minimum energy structures were performed as follows. The alkali-metal hexatitanates were minimized using two steps: (1) the octahedral titaniums were relaxed while the interlayer alkali-metal ions were kept fixed, and (2) all the ions were relaxed simultaneously relative to a fixed titanium ion until the total energies were converged. For the systems with ruthenium oxide we optimized the structure both before and after incorporation. Relaxations were continued until the total energy had converged. A cluster was designed from the hexatitanate structure with formula $M_2Ti_2O_{11}H_{12}$, where $M = Na, K, \text{ or } Rb$. Except the bridging Ti–O–Ti bond all the

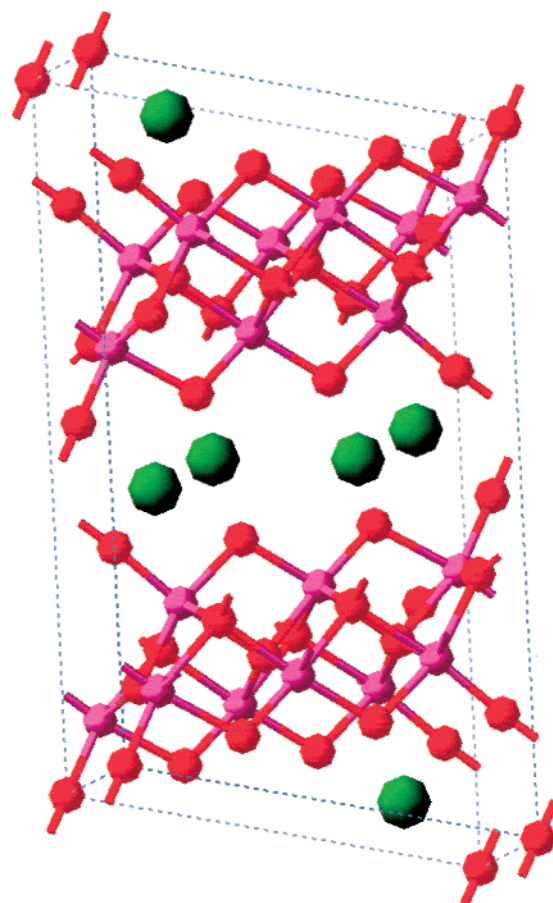


Figure 1. The general structure of alkali-metal hexatitanate. The color code is as follows: red, oxygen; pink, titanium; green, alkali metal.

titaniums in the structure was replaced by hydrogen for electrical neutrality. The hydrogens were kept at the titanium positions and kept fixed throughout the calculation. The cluster model is shown in Figure 2.

Results and Discussion

Our aim is to rationalize the location and role of ruthenium oxide in the photocatalytic activity of the alkali-metal hexatitanates. To achieve this first we optimized the structures of alkali-metal (Na, K, Rb) hexatitanates to validate our model. This is followed by localized cluster calculations to monitor the most favorable conformation of the ruthenium oxide inside hexatitanates and to find the best candidate to accommodate ruthenium oxide. Then, periodic structures of the ruthenium oxide incorporated hexatitanates are optimized; the geometry and the structural parameters were compared. Finally, the density of state calculation has been performed on Na-hexatitanate, with and without ruthenium oxide incorporation to compare the role of ruthenium oxide in photocatalysis.

a. Comparison of Structure and Geometry of Alkali-Metal Hexatitanates Using CASTEP. The general structure of alkali-metal hexatitanate is shown in Figure 1. Here the alkali metal is sodium. Each of the three hexatitanate structures has been minimized with the same cut-off energy of 600 eV and with two k points in the Brillouin zone. Now from the crystal structure³ it is known that, the hexatitanates are a framework of titanium and oxygen atoms, which encapsulates the alkali-metal cation. Each titanium has six oxygen neighbors at the corners of a distorted octahedron. Now the octahedras are joined above and below to similar groups by further edge sharing and form a zigzag ribbon extending in the y -direction. This results

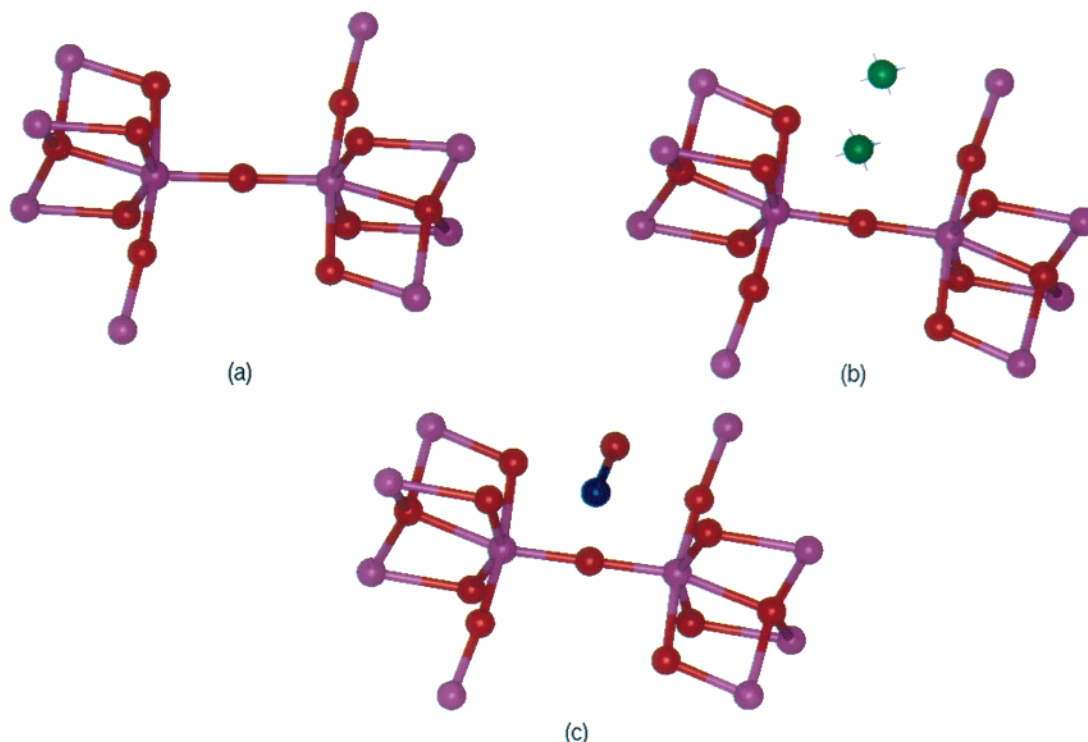


Figure 2. The cluster model designed from the hexatitanate structure (a) with formula $\text{Ti}_2\text{O}_{11}\text{H}_{12}$ formula representing hexatitanate, (b) with formula $\text{M}_2\text{Ti}_2\text{O}_{11}\text{H}_{12}$ representing alkali-metal hexatitanate where $\text{M} = \text{Na}, \text{K}, \text{Rb}$ (c) with formula $(\text{RuO})\text{Ti}_2\text{O}_{11}\text{H}_{12}$.

in an open octahedral framework with tunnels in which the alkali-metal cations are located. The cell-parameters and internal coordinates are presented in Table 1 for Na, K, and Rb hexatitanate. The bond lengths along with standard deviation are presented in Table 2. It is observed that the Ti–O distances vary from 1.819 to 2.108 Å. This is in agreement with the experimental numbers.³ There is some variation in the O–O distances; with the shortest ranging from 2.42 to 2.51, corresponding to pairs, which are common to two adjacent titanium atoms. The results are in agreement with experimental values.³ This validates our methodology. The lengths of a and b axes of the alkali-metal hexatitanates increase in the order $\text{Na} \rightarrow \text{K} \rightarrow \text{Rb}$ as expected but the c axial length shows a corresponding decrease. Due to the elongation in a and b axis and a corresponding decrease in c axial length some individual atoms change considerably to accommodate the enlargement inside the tunnels. O5 being the worst affected, the O4–O5 distance changes from 2.48 for Na-hexatitanate to 2.29 for Rb-hexatitanate. The distortion in titanium octahedral results in a distortion in the tunnel structure. This distortion further influences the location of the alkali metal inside the tunnel. These results show that the structures of the hexatitanate have some differences in structural and geometric parameters depending on the nature of the alkali-metal cation. The experimental order of stability and elongation and depression of axes are validated which justifies the model as well. Now to monitor the influence of alkali metals on the location of ruthenium oxide we performed localized cluster calculation.

b. Localized Cluster Calculations with DFT to Monitor the Influence of Alkali-Metal Cation on Location of Ruthenium Oxide. To predict the location of ruthenium oxide in alkali-metal hexatitanate, we performed localized cluster calculations.⁴² Now, in hexatitanate each titanium has six oxygen neighbors at the corners of a distorted octahedron. The octahedral share edges resulting in an open octahedral framework enclosing tunnels in which the sodium ions are located.

To achieve our primary aim of rationalizing the location of ruthenium oxide in hexatitanates and to explore the situation in a smaller scale we need to have a cluster containing Ti–O–Ti bridge, which lies closer to the metal cation, and where the environment of the metal ion and the titanium can be same as in the compound. We designed the cluster from the well-defined crystal structure of sodium hexatitanate. We have used a generalized cluster formula $\text{M}_2\text{Ti}_2\text{O}_{11}\text{H}_{12}$, where $\text{M} = \text{Na}, \text{K},$ or Rb . The terminal titaniums are replaced by hydrogen for electrical neutrality of the cluster. Now the two titaniums present in the cluster are octahedrally coordinated. The sodium is located near to the oxygen connecting two titaniums in the cluster. The cluster models representing bare hexatitanate, alkali-metal hexatitanate, and ruthenium oxide exchanged hexatitanate are shown in Figure 2, parts a, b, and c, respectively. Now if we substitute two alkali metals present in the cluster by ruthenium oxide, it can be done in following two ways:



For the first case the formal oxidation state of ruthenium is VI, which is not likely to happen, as experimentally it is observed that the oxidation state of ruthenium is IV.⁴ But, the second route seems probable. Thus, we used the second equation to calculate the relative substitution energy for different alkali metals in their respective hexatitanates. The substitution energy values for hexatitanates falls in the order $\text{Na} < \text{K} < \text{Rb}$. The Mulliken population analysis at this optimized cluster shows the average charge density on ruthenium and oxygen is more negative with respect to the titanium and oxygen of the bulk, showing its feasibility toward photoexcitation. The localization of negative charge will favor the dipole–dipole interaction, which in otherway will enhance the photocatalytic activity. It shows that for sodium hexatitanate the relative substitution

TABLE 1: Cell Parameters and Internal Coordinates for Optimized Sodium Hexatitanate, Potassium Hexatitanate, and Rubidium Hexatitanate Using CASTEP

name	X	Y	Z
Optimized Sodium Hexatitanate ^{a,b}			
Ti1	0.11498 (0.11370)	0.00000	0.09518 (0.08950)
Ti2	0.16612 (0.17050)	0.00000	0.43493 (0.43320)
Ti3	0.22620 (0.22870)	0.00000	0.77010 (0.77260)
Na1	0.45727 (0.45400)	0.00000	0.26130 (0.25080)
O1	0.00000 (0.00000)	0.00000	0.00000 (0.00000)
O2	0.24238 (0.22800)	0.00000	0.24540 (0.24700)
O3	0.07118 (0.07100)	0.00000	0.28878 (0.29100)
O4	0.29780 (0.28200)	0.00000	0.57145 (0.57400)
O5	0.12711 (0.12400)	0.00000	0.61123 (0.61700)
O6	0.35484 (0.35800)	0.00000	0.88660 (0.88400)
O7	0.15927 (0.16700)	0.00000	0.90782 (0.92700)
Optimized Potassium Hexatitanate ^{c,d}			
Ti1	0.11442	0.00000	0.09408
Ti2	0.16689	0.00000	0.43448
Ti3	0.22701	0.00000	0.77152
K1	0.45686	0.00000	0.26059
O1	0.00000	0.00000	0.00000
O2	0.24107	0.00000	0.24347
O3	0.07249	0.00000	0.28896
O4	0.29716	0.00000	0.57202
O5	0.12922	0.00000	0.61176
O6	0.35515	0.00000	0.88777
O7	0.15957	0.00000	0.90765
Optimized Rubidium Hexatitanate ^{c,b}			
Ti1	0.11432 (0.114)	0.00000	0.09393 (0.093)
Ti2	0.17361 (0.174)	0.00000	0.43621 (0.435)
Ti3	0.23350 (0.236)	0.00000	0.77757 (0.778)
Rb1	0.45550 (0.456)	0.00000	0.25521 (0.250)
O1	0.00000 (0.000)	0.00000	0.00000 (0.000)
O2	0.23992 (0.233)	0.00000	0.23865 (0.237)
O3	0.08123 (0.084)	0.00000	0.28978 (0.305)
O4	0.29679 (0.273)	0.00000	0.57216 (0.577)
O5	0.13797 (0.134)	0.00000	0.61417 (0.612)
O6	0.35824 (0.351)	0.00000	0.88886 (0.908)
O7	0.16664 (0.165)	0.00000	0.91372 (0.919)

^a $a = 15.232$ (15.131), $b = 3.843$ (3.745), $c = 9.29$ (9.159); $\alpha = \gamma = 90.0$, $\beta = 99.49$ (99.3). Symmetry group: $C2/m$ monoclinic.

^b Numbers in the parentheses are the experimental values. ^c $a = 15.770$ (15.600), $b = 3.921$ (3.800), $c = 9.26$ (9.130); $\alpha = \gamma = 90.0$, $\beta = 99.71$ (99.60). Symmetry group: $C2/m$ monoclinic. ^d Numbers in the parentheses are the experimental values. No experimental values are available for fractional coordinates. ^e $a = 16.080$ (15.890), $b = 3.962$ (3.820), $c = 9.22$ (9.110); $\alpha = \gamma = 90.0$, $\beta = 100.47$ (100.4). Symmetry group: $C2/m$ monoclinic.

energy for ruthenium oxide substitution is the lowest or in other way it states that sodium hexatitanate will be the best candidate available for the substitution of ruthenium oxide by ion exchange. The difference of energy is in the range of 8–15 kcal/mol. These numbers don't have any quantitative significance, but qualitatively a trend can be achieved. We may say that Na-hexatitanate behaves as a better candidate among the others in terms of exchanging ruthenium oxide. It is also observed that the ruthenium oxide moiety lies in such a way that the oxygen atom is tilted toward the oxygens of the titanium. This proposes that the ruthenium oxide fits the location of the sodium in its special geometry. As it is known from the structure of sodium-hexatitanate,³ the sodium atom has a pseudo octahedral coordination with the surrounding oxygen and the ruthenium oxide places itself in that particular orientation. Hence, the ruthenium may fit into the tunnel environment with some disorder.

c. Proposed Location of Ruthenium Oxide inside Alkali-Metal Hexatitanate Using CASTEP. The X-ray photoelectron spectra⁴ of Ru deposited on sodium hexatitanate shows that the

TABLE 2: Bond Lengths for Optimized Alkali-Metal Hexatitanates Using CASTEP^a

Ti-O				M-O, where M = Na, K, Rb							
bond				O-O							
length	Na-t	K-t	Rb-t	Na-t	K-t	Rb-t	Na-t	K-t	Rb-t		
Ti1-O1	1.78	1.82	1.85	O1-O7	2.72	2.79	2.85	M-O3	2.56	2.62	2.77
Ti1-O2	2.06	2.09	2.10	O7-O2	3.02	3.11	3.02	M-O5	2.61	2.65	2.81
Ti1-O3	2.05	2.06	2.07	O2-O3	2.47	2.55	2.55	M-O7	2.92	2.96	2.94
Ti1-O7	1.92	1.95	1.99	O1-O3	2.71	2.70	2.86	M-O1	3.13	3.14	3.15
Ti1-O6	1.89	1.91	1.93	O1-O6	2.92	2.98	3.04	S	0.19	0.16	0.17
S	0.11	0.12	0.11	O7-O6	2.98	3.07	2.97				
Ti2-O2	2.03	2.05	2.18	O2-O6	2.48	2.51	2.56				
Ti2-O3	1.82	1.85	1.68	O3-O6	2.79	2.82	3.03				
Ti2-O4	1.95	1.98	1.85	O2-O3	2.42	2.55	2.55				
Ti2-O5	1.92	1.94	1.84	O2-O4	2.51	2.53	2.57				
Ti2-O4	2.01	2.04	2.09	O4-O5	2.48	3.11	3.12				
S	0.08	0.08	0.09	O3-O5	2.96	2.95	2.77				
Ti3-O4	2.11	2.12	2.02	O2-O4	2.51	2.53	2.57				
Ti3-O5	1.95	1.98	2.01	O3-O4	3.02	3.07	3.01				
Ti3-O6	2.05	2.10	1.98	O4-O4	2.42	2.45	2.40				
Ti3-O7	1.82	1.83	1.86	O5-O4	3.06	3.11	3.12				
Ti3-O2	2.00	2.03	1.98	O4-O5	2.48	2.56	2.29				
S	0.11	0.11	0.10	O4-O6	2.89	2.88	3.05				
				O6-O7	2.98	3.07	2.97				
				O5-O7	2.81	2.80	2.75				
				O4-O2	2.51	2.53	2.57				
				O6-O2	2.48	2.51	2.56				
				O7-O2	3.06	3.11	3.02				
				O5-O2	3.03	3.09	2.99				
				S	0.21	0.20	0.19				

^a S = standard deviation, Na-t, K-t and Rb-t are Na-hexatitanate, K-hexatitanate and Rb-hexatitanate, respectively.

binding energy of Ru 3d_{5/2} level of the photocatalysts treated by reduction was similar to that of metallic Ru, where as the oxidation led to a binding energy level close to that observed for RuO₂ powder and oxidized Ru metal. This indicates that Ru exists in a chemical form analogous to RuO₂ and indicates that Ru(IV) is the active species present. So chemically there is an exchange of alkali-metal cation by ruthenium followed by its oxidation. Experimentally⁴ it is observed that when sodium hexatitanate is immersed in RuCl₃ solution, the ratio of liberated Na ions and deposited Ru ions is ~2. The amount of Na ions replaced corresponds to at least nine layers of the titanate at 0.23% Ru content. This indicates that the intercalation of Ru is deep inside the titanate and not in the surface. The mechanism is as follows:



where M = Na, K, Rb.

Then RuCl gets oxidized to a ruthenium oxide, Ru(IV). The experimentalist observed that the photocatalytic activity increased almost proportionally with the content of Ru species up to a maximum of 0.23 wt %. These results make the experimentalists believe that Ru is also deposited inside the titanate as well as on the surface. Now the decrease in the photocatalytic activity with an excess of Ru loading was explained in terms of agglomeration and deactivation of the active Ru(IV) centers.⁴³ The location of the ruthenium oxide is not known experimentally and so its role is yet to be confirmed.

From the localized cluster calculation we observed that the ruthenium oxide gets stabilized closer to the oxygen linked with titanium inside the tunnel, so we inserted the ruthenium oxide moiety in the tunnel formed by titanium oxide octahedrals and relaxed it. Now ruthenium oxide insertion can take place in two ways: (1) exchange of all of the alkali-metal cations (i.e., after exchange there will not be any alkali-metal cation), and (2) a

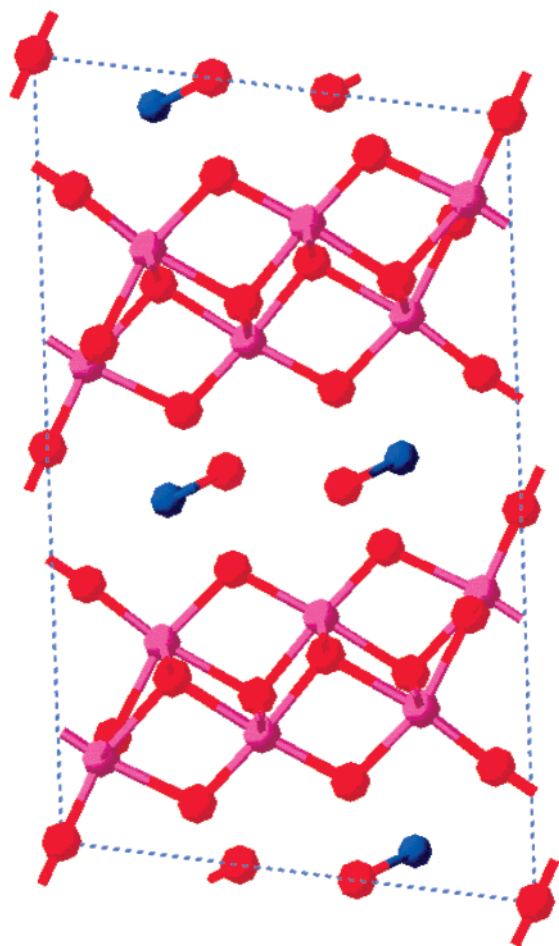


Figure 3. The structure of sodium hexatitanate with all of its sodium is replaced by ruthenium oxide. The color code is as follows: red, oxygen; pink, titanium; green, sodium; blue, ruthenium.

TABLE 3: Cell Parameters in Å for Hexatitanates before and after Incorporation of Ruthenium Oxide Using CASTEP^a

cell param- eters	initial ^b	relaxation before incorporation	dif- ference	relaxation after incorporation	dif- ference
<i>a</i>	(i) 15.131 (ii) 15.600 (iii) 15.890	15.232 15.770 16.080	0.1 0.17 0.19	16.61 16.45 16.45	1.47 0.85 0.56
<i>b</i>	(i) 3.745 (ii) 3.800 (iii) 3.820	3.843 3.921 3.962	0.098 0.121 0.142	3.68 3.75 3.79	0.06 0.05 0.03
<i>c</i>	(i) 9.159 (ii) 9.130 (iii) 9.110	9.29 9.26 9.22	0.14 0.13 0.11	9.72 9.57 9.37	0.56 0.44 0.26
β	(i) 99.30 (ii) 99.60 (iii) 100.4	99.49 99.71 100.47	0.19 0.11 0.07	104.21 103.91 102.74	4.91 4.31 2.34

^a Average % of ruthenium oxide incorporation with respect to the metal cation is 50%. ^b (i) Sodium hexatitanate; (ii) Potassium hexatitanate; (iii) Rubidium hexatitanate.

few of the metal cations are exchanged by ruthenium oxide (i.e., there will remain few unreacted alkali-metal cation). A situation where all the metal cations were exchanged by ruthenium oxide is shown in Figure 3. We mimic a situation with 50% ruthenium oxide incorporation to depict the condition (2), which is shown in Figure 4. The structural parameters have been calculated. The results have been monitored in two steps—first, before incorporation of ruthenium oxide, and second, after incorporation of ruthenium oxide. The results are shown in Table 3. For

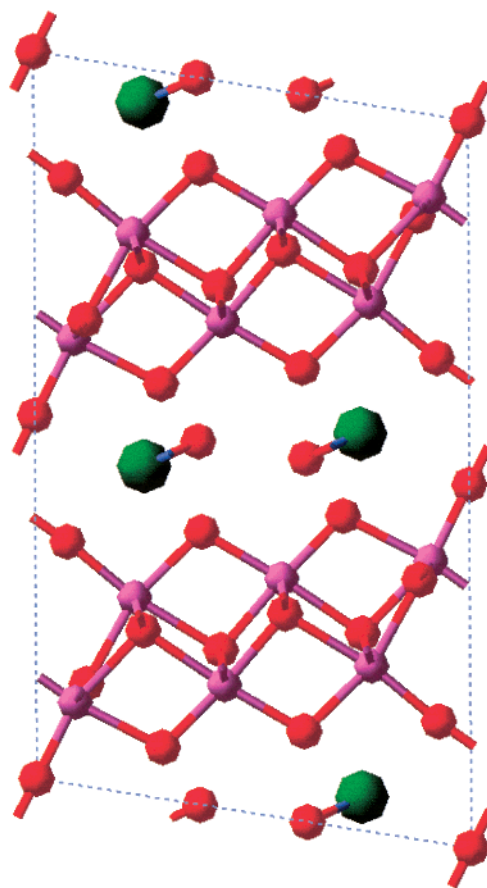


Figure 4. The structure of sodium hexatitanate with 50% of its sodium replaced by ruthenium oxide. The color code is as follows: red, oxygen; pink, titanium; blue, ruthenium; green, sodium.

TABLE 4: Internal Coordinates for Optimized Ruthenium Oxide Hexatitanate, Where Ruthenium Oxide Has Been Incorporated in Place of Sodium^{a,b}

name	X	Y	Z
Ti1	0.11366 (0.11370)	0.00000	0.07776 (0.08950)
Ti2	0.17647 (0.17050)	0.00000	0.42938 (0.43320)
Ti3	0.22435 (0.22870)	0.00000	0.76796 (0.77260)
Ru1	0.41377 (0.45400)	0.00000	0.22083 (0.25080)
O8	-0.51704	0.67808	0.34128
O1	0.00000 (0.00000)	0.00000	0.00000 (0.00000)
O2	0.25141 (0.22800)	0.00000	0.23194 (0.24700)
O3	0.10197 (0.07100)	0.00000	0.25680 (0.29100)
O4	0.29173 (0.28200)	0.00000	0.58085 (0.57400)
O5	0.14252 (0.12400)	0.00000	0.58989 (0.61700)
O6	0.34168 (0.35800)	0.00000	0.90754 (0.88400)
O7	0.14339 (0.16700)	0.00000	0.87684 (0.92700)

^a Numbers in the parenthesis are the experimental values. ^b $a = 16.61$ (15.131), $b = 3.68$ (3.745), $c = 9.72$ (9.159); $\alpha = \gamma = 90.0$, $\beta = 104.21$ (99.3). Symmetry group: $C2/m$ monoclinic.

the first case, i.e., before incorporation of ruthenium dioxide, a and b parameters increase and c parameter decreases for the hexatitanates in the order $\text{Na} \rightarrow \text{K} \rightarrow \text{Rb}$. The general trend before incorporation of ruthenium oxide (RuO) is in perfect match with the experimental observation as it is mentioned earlier as well. But the interesting point is after the incorporation of ruthenium oxide (RuO) the increment of cell parameter in comparison to the initial situation is drastic. The trend also changes. It is observed that after ruthenium oxide incorporation, the a and c parameters decrease and the b parameter increases in the order $\text{Na} \rightarrow \text{K} \rightarrow \text{Rb}$. The individual increment in cell parameters is much more pronounced in comparison to the

TABLE 5: Bond Lengths of Optimized Ruthenium Oxide Exchanged Hexatitanates Using CASTEP^a

Ru–O				O–O				Ru–O intramolecular			
atom number	Na-t	K-t	Rb-t	atom number	Na-t	K-t	Rb-t	atom number	Na-t	K-t	Rb-t
Ru–O3	2.64	2.62	2.61	O8–O3	1.63	1.61	1.58	Ru–O8	1.74	1.74	1.74
Ru–O5	2.66	2.65	2.64	O8–O5	2.08	2.06	2.02				
Ru–O7	2.98	2.96	2.92	O8–O7	3.52	3.53	3.47				
Ru–O1	3.16	3.14	3.12	O8–O1	3.54	3.50	3.48				
S	0.11	0.12	0.11	S	0.13	0.14	0.12				

^a S = Standard deviation. Na-t, K-t and Rb-t are Na-hexatitanate, K-hexatitanate, and Rb-hexatitanate, respectively.

situation without ruthenium oxide. The difference is much more pronounced for *a* and *b* parameters whereas for *c* parameters the difference from the initial situation is less. The expansion is highest in the case of sodium hexatitanate followed by potassium and rubidium. This means that for the larger alkali-metal ion, the ion exchange reaction between alkali metal and RuO is suppressed due to the distortion of the tunnel structure of the hexatitanate. Hence, an ion exchange reaction should be easier for sodium hexatitanate than for rubidium hexatitanate. This also induces a feeling that the extent of distortion of the tunnel framework negatively influences the efficiency of photoexcitation. The whole effect is over the TiO₆ octahedra, which get expanded, or which shrink, depending on the presence of the alkali-metal cation. This is clearly observed in the geometry of the lattice. The O–O distance, which forms the edges, has been reduced from 0.25 nm of sodium hexatitanate to 0.21 nm in the case of rubidium hexatitanate. This is in agreement with the X-ray crystal data.⁴ The substitution energy results after incorporation of ruthenium oxide follows the same trend with that obtained without incorporation. Sodium hexatitanates get more stabilized after ruthenium oxide incorporation. The present results suggest that structural differences are probably responsible for the different photocatalytic properties. Sodium-hexatitanate is the best among all the hexatitanates studied for photocatalytic behavior in the presence of ruthenium oxide.

The atomic coordinates for ruthenium oxide exchanged alkali-metal hexatitanates are shown in Table 4. The distortion resulted in the framework of hexatitanates proposes that RuO may be located inside the tunnel structure. The bond lengths of the ruthenium oxide exchanged hexatitanates with standard deviations are given in Table 5. The results show clearly that with 100% exchange of ruthenium oxide, Na-hexatitanate present itself as the best candidate for the process. In the case with 50% exchange of ruthenium oxide the results do not show much difference with the 100% exchange situation. The location of ruthenium oxide inside the tunnel structure also explains the phenomenon of membrane effect of the titanates, which allows not only the separation of charges but also separation of reaction products. The atomic coordinates and the cell parameter for the ruthenium oxide incorporated hexatitanate structures are thus established. The surface agglomeration of ruthenium is beyond the scope of the article. We can say that if ruthenium oxide is formed by ion exchange and oxidation, then it should be located inside the tunnel. The ruthenium moiety, which lies on the surface could be the metallic ruthenium, as when we tried the relaxation by placing the ruthenium oxide moiety on the surface it did not seem to be stable. This is due to the strong repulsion between surface oxygen and the oxygen of ruthenium oxide. The situation changed when we tried with metallic ruthenium. It got stabilized on the surface, locating itself out of the oxide plane.

d. Density of States for Ruthenium Oxide Exchanged and Unexchanged Sodium Hexatitanates. The density of states (DOS) calculations have been performed on sodium hexatitanate

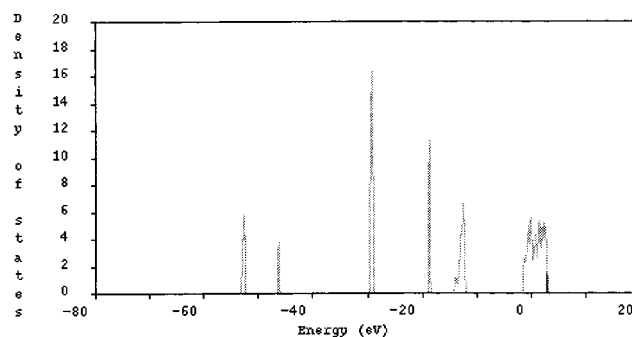


Figure 5. Total density of state for sodium hexatitanate. The gap shown here is between O 2p and Ti 3d.

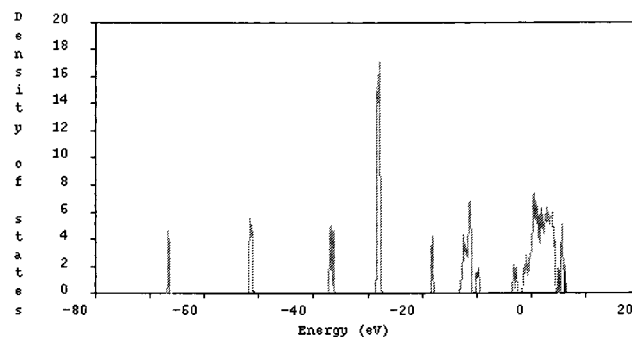


Figure 6. Total density of state for sodium hexatitanate. The gap shown here is between O 2p and Ru 3d.

both exchanged and unexchanged with ruthenium oxide. The results are shown in Figure 5 and Figure 6, respectively. It is observed that after ruthenium oxide incorporation the DOS shifted upward in energy. Now for the hexatitanate if an electron is excited from an O 2p orbital to a Ti 3d orbital, then the energy gap is 2.85 eV. But when ruthenium oxide is incorporated then the energy gap is much lower as clearly visible in Figure 6. At the same time there exists a broadening of the band. Now it is well-known that for metallic d bands, a rigid band model describes the 4d ruthenium oxide material.⁴⁴ Here in case of ruthenium oxide exchanged hexatitanate the transition occurs between O 2p and Ru 3d 5/2. The energy gap is 0.78 eV. This is close to the chemical shift value observed experimentally 0.6 eV. This shows clearly that after ruthenium oxide incorporation the activity enhancement is reasonable. Hence the experimental observation regarding activity toward photocatalysis for hexatitanates after ruthenium oxide exchange is explained. This ruthenium oxide is located inside the tunnel of the hexatitanate structure and has photocatalytic activity. This also validates the observation of previous studies on the behavior of mixed metal oxides.^{25,30} The electronic states induced by RuO above the hexatitanate valence band had a strong impact on the chemical properties of the material. An important factor governing the ruthenium oxide activity could be the alkali-metal cation present. The alkali-metal cation dictates the location of the oxide moiety inside the structure, which is especially favored inside the Na-

hexatitanate due to favorable expansion and distortion of the tunnel environment.

Conclusions and Summary

This is the first study to rationalize the location and activity of ruthenium oxide incorporated into alkali-metal hexatitanates. We used two different methodologies to examine the problem. First the CASTEP results with bare hexatitanates show that the best candidate among other hexatitanates is that with sodium. Localized cluster calculations were useful to propose the location of ruthenium oxide inside the hexatitanate in a qualitative way. Our results show that if the ruthenium is present as oxide it should reside inside the tunnel structure of the hexatitanates. Ruthenium oxide can never be stabilized on the surface due to dipole–dipole repulsion. The surface may contain metallic ruthenium. The density of states calculation plots with and without ruthenium oxide revealed the fact that structures with ruthenium oxide are more active toward photocatalysis in comparison to bare hexatitanate. This validates the experimental observations. Also an expansion in the lattice shows that the feasibility of photocatalytic activity is favored after the inclusion of ruthenium oxide. Our cluster calculations also reveal the fact that the charge distribution allows the ruthenium oxide to be the active species in photocatalytic reactions in hexatitanates. We were also successful in predicting the structure of ruthenium oxide inside the hexatitanate tunnel. Our methodology could be useful for studying similar problems with other inorganic systems where a structure property correlation is yet to be achieved.

References and Notes

- (1) Richardson, M. O. *Polymer Engineering Composites*; International Ideas: Philadelphia, 1977.
- (2) Gullledge, H. C. *Ind. Eng. Chem.* **1960**, *52*, 117.
- (3) Andersson, S.; Wadsley, A. D. *Acta Crystallogr.* **1962**, *15*, 194.
- (4) Inoue, Y.; Kubokawa, T.; Sato, K. *J. Phys. Chem.* **1991**, *95*, 4059.
- (5) Kudo, A.; Tanaka, A.; Domen, K.; Maruya, K.; Akita, K.; Onishi, T. *J. Catal.* **1988**, *111*, 67.
- (6) Tanaka, T.; Furumi, Y.; Shinohara, K.; Tanaka, A.; Hara, M.; Kondo, J. N.; Domen, K. *Chem. Mater.* **1997**, *9*, 1063.
- (7) Ebina, Y.; Tanaka, A.; Kondo, J. N.; Domen, K. *Chem. Mater.* **1996**, *8*, 2534.
- (8) Inoue, Y.; Kubokawa, T.; Sato, K. *J. Chem. Soc. Chem. Commun.* **1990**, 128.
- (9) Ogura, S.; Kohno, M.; Sato, K.; Inoue, Y. *Phys. Chem. Chem. Phys.* **1999**, *1*, 179.
- (10) Causa, M.; Dovesi, R.; Pisani, C.; Roetti, C. *Surf. Sci.* **1986**, *175*, 551.
- (11) Scafehorn, C. A.; Hess, A. C.; McCarthy, M. I. *J. Chem. Phys.* **1993**, *99*, 2786.
- (12) McCarthy, M. I.; Hess, A. C.; Harrison, N. M.; Saunders, V. R. *J. Chem. Phys.* **1993**, *98*, 6387.
- (13) Jaffe, J. E.; Harrison, N. M.; Hess, A. C. *Phys. Rev. B* **1994**, *49*, 11153.
- (14) Rehbein, C.; Harrison, N. M.; Wander, A. *Phys. Rev. B* **1996**, *54*, 14066.
- (15) Mackrodt, W. C.; Simson, E.-A.; Harrison, N. M. *Surf. Sci.* **1997**, *384*, 192.
- (16) Kantrovich, L. N.; Holender, J. M.; Gillian, M. J. *Surf. Sci.* **1995**, *343*, 221.
- (17) Langel, W.; Parrinello, M. *Phys. Rev. Lett.* **1994**, *73*, 504.
- (18) Manassidis, I.; Gillian, M. J. *J. Am. Ceram. Soc.* **1994**, *77*, 335.
- (19) Manassidis, I.; Goniakowski, J.; Kantorovich, L. N.; Gillian, M. J. *Surf. Sci.* **1995**, *339*, 258.
- (20) Lindan, P. J. D.; Muscat, J.; Bates, S.; Harrison, N. M.; Gillan, M. *Faraday Discuss.* **1997**, *106*, 135.
- (21) Ramamoorthy, M.; Vanderbilt, D.; King-Smith, R. D. *Phys. Rev. B* **1994**, *49*, 16721.
- (22) Goniakowski, J.; Holender, J. M.; Kantorovich, L. N.; Gillian, M. J.; White, J. A. *Phys. Rev. B* **1996**, *53*, 957.
- (23) Lindan, P. J. D.; Harrison, N. M.; White, J. A.; Gillan, M. J. *Phys. Rev. B* **1997**, *55*, 15919.
- (24) Rodriguez, J. A.; Jirsak, T.; Sambasivan, S.; Fischer, D.; Maiti, A. *J. Chem. Phys.* **2000**, *112*, 9929.
- (25) Rodriguez, J. A.; Jirsak, T.; Pérez, M.; Chaturvedi, S.; Kuhn, M.; González, L.; Maiti, A. *J. Am. Chem. Soc.* **2000**, *122*, 12362.
- (26) Sorescu, D. C.; Yates, J. T., Jr. *J. Phys. Chem. B* **1998**, *102*, 4556.
- (27) Sorescu, D. C.; Rusu, C. N.; Yates, J. T., Jr. *J. Phys. Chem. B* **2000**, *104*, 4408.
- (28) Snyder, J. A.; Alfonso, D. R.; Jaffe, J. E.; Lin, Z.; Hess, A. C.; Gutowski, M. J. *J. Phys. Chem. B* **2000**, *104*, 4717.
- (29) Rodriguez, J. A.; Hanson, J. C.; Chaturvedi, S.; Maiti, A.; Brito, J. L. *J. Chem. Phys.* **2000**, *112*, 935.
- (30) Rodriguez, J. A.; Hanson, J. C.; Chaturvedi, S.; Maiti, A.; Brito, J. *Phys. Chem. B* **2000**, *104*, 8145.
- (31) Chatterjee, A.; Iwasaki, T.; Ebina, T. *J. Phys. Chem. A* **2000**, *104*, 8216.
- (32) Teter, M. P.; Payne, M. C.; Allen, D. C. *Phys. Rev. B* **1989**, *40*, 12255.
- (33) Payne, M. C.; Teter, M. P.; Allen, D. C.; Arias, T. A.; Johannopoulos, J. D. *Rev. Modern. Phys.* **1992**, *64*, 1045.
- (34) Vanderbilt, D. *Phys. Rev. B* **1990**, *41*, 7892.
- (35) Monkhorst, H. J.; Pack, J. D. *Phys. Rev. B* **1976**, *13*, 5188.
- (36) (a) Perdew, J. P.; Wang, Y. *Phys. Rev. B* **1992**, *46*, 6671. (b) White, J. A.; Bird, D. M. *Phys. Rev. B* **1994**, *50*, 4954.
- (37) Kohn, W.; Sham, L. J. *Phys. Rev. A* **1965**, *140*, 1133.
- (38) Becke, A. J. *Chem. Phys.* **1988**, *88*, 2547.
- (39) Leu, C.; Yang, W.; Parr, R. G. *Phys. Rev. B* **1988**, *37*, 786.
- (40) Bock, C. W.; Trachtman, M. *J. Phys. Chem.* **1994**, *98*, 95.
- (41) Berry, K. L.; Aftandilian, V. D.; Gilbert, W. W.; Meibohm, E. P. H.; Young, H. S. *J. Inorg. Nucl. Chem.* **1960**, *14*, 231.
- (42) Derouane, E. G.; Fripiat, J. G. *Zeolites* **1985**, *5*, 165.
- (43) Sakata, T.; Hashimoto, K.; Kawai, T. *J. Phys. Chem.* **1984**, *88*, 5214.
- (44) Xu, J. H.; Jarlbary, T.; Freeman, A. J. *Phys. Rev. B* **1989**, *40*, 7937.